



# Clinical Yield of Magnetoencephalography Distributed Source Imaging in Epilepsy: A Comparison With Equivalent Current Dipole Method

Giovanni Pellegrino <sup>1,2,3\*</sup>, Tanguy Hedrich,<sup>1</sup>  
Rasheda Arman Chowdhury <sup>1</sup>, Jeffery A. Hall,<sup>2</sup> Francois Dubeau,<sup>2</sup>  
Jean-Marc Lina,<sup>4,5,6</sup> Eliane Kobayashi,<sup>2</sup> and Christophe Grova<sup>1,2,5,7</sup>

<sup>1</sup>Multimodal Functional Imaging Lab, Biomedical Engineering Department, McGill University, Montreal, Quebec, Canada

<sup>2</sup>Neurology and Neurosurgery Department, Montreal Neurological Institute, McGill University, Montreal, Quebec, Canada

<sup>3</sup>IRCCS Fondazione San Camillo Hospital, Venice, Italy

<sup>4</sup>Departement de Génie Electrique, Ecole de Technologie Supérieure, Montreal, Quebec, Canada

<sup>5</sup>Centre De Recherches En Mathématiques, Montreal, Quebec, Canada

<sup>6</sup>Centre D'études Avancées En Médecine Du Sommeil, Centre De Recherche De L'hôpital Sacré-Coeur De Montréal, Montreal, Quebec, Canada

<sup>7</sup>Physics Department and PERFORM Centre, Concordia University, Montreal, Quebec, Canada



**Abstract:** *Objective:* Source localization of interictal epileptic discharges (IEDs) is clinically useful in the presurgical workup of epilepsy patients. It is usually obtained by equivalent current dipole (ECD) which localizes a point source and is the only inverse solution approved by clinical guidelines. In contrast, magnetic source imaging using distributed methods (dMSI) provides maps of the location and the extent of the generators, but its yield has not been clinically validated. We systematically compared ECD versus dMSI performed using coherent Maximum Entropy on the Mean (cMEM), a method sensitive to the spatial extent of the generators. *Methods:* 340 source localizations of IEDs derived from 49 focal epilepsy patients with foci well-defined through intracranial EEG, MRI lesions, and surgery were analyzed. The comparison was based on the assessment of the sublobar concordance with the focus

Additional Supporting Information may be found in the online version of this article.

Institution at which the work was performed: Montreal Neurological Institute (MNI) and Biomedical Engineering Department, McGill University, Montreal, QC, Canada.

Contract grant sponsor: Canadian Institutes of Health Research; Contract grant number: MOP-93614; Contract grant sponsor: Natural Sciences and Engineering Research Council of Canada; Contract grant sponsor: Fonds de Recherche du Québec – Santé; Contract grant sponsor: Academic Center for Education, Culture and Research; Contract grant sponsor: Canadian Network for Research and Innovation in Machining Technology; Contract

grant sponsor: American Epilepsy Society; Contract grant sponsor: Richard and Edith Strauss Canada Foundation.

\*Correspondence to: Giovanni Pellegrino, MD; 332 Duff Medical Building, 3775 University Street, Montreal, QC H3A2B4, Canada. E-mail: giovannipellegrino@gmail.com

Received for publication 27 April 2017; Revised 25 August 2017; Accepted 25 September 2017.

DOI: 10.1002/hbm.23837

Published online 11 October 2017 in Wiley Online Library (wileyonlinelibrary.com).

and of the distance between the source and the focus. *Results:* dMSI sublobar concordance was significantly higher than ECD (81% vs 69%,  $P < 0.001$ ), especially for extratemporal lobe sources (dMSI = 84%; ECD = 67%,  $P < 0.001$ ) and for seizure free patients (dMSI = 83%; ECD = 70%,  $P < 0.001$ ). The median distance from the focus was 4.88 mm for ECD and 3.44 mm for dMSI ( $P < 0.001$ ). ECD dipoles were often wrongly localized in deep brain regions. *Conclusions:* dMSI using cMEM exhibited better accuracy. dMSI also offered the advantage of recovering more realistic maps of the generator, which could be exploited for neuronavigation aimed at targeting invasive EEG and surgical resection. Therefore, dMSI may be preferred to ECD in clinical practice. *Hum Brain Mapp* 39:218–231, 2018. © 2017 Wiley Periodicals, Inc.

**Key words:** interictal epileptiform discharges; source localization; MEG; presurgical evaluation; dipole; magnetic source imaging; surgery; distributed source; spike

## INTRODUCTION

Magnetoencephalography (MEG) source localization can improve the placement of intracranial EEG electrodes (iEEG) and guide cortical resection in drug-resistant epilepsy patients [Knowlton et al., 2006; Ryvlin et al., 2014; Stefan et al., 2003].

Localizing the generator of interictal epileptiform discharges (IEDs) from MEG recordings consists in solving an ill-posed inverse problem. Several source localization techniques have been proposed such as equivalent current dipole (ECD) or distributed magnetic source imaging (dMSI) [Dale and Sereno, 1993; Darvas et al., 2004]. However, ECD method is the only method clinically validated and approved [Bagic et al., 2011; Barth et al., 1982; Bast et al., 2004; Knowlton et al., 1997; Stefan et al., 2003]. ECD assumes that IEDs are generated by point sources, characterized by three spatial coordinates, a magnitude and an orientation [Scherg and Von Cramon, 1985]. It is operator-dependent and can provide misleading localizations when the signal to noise ratio is low or when the epileptic focus is spatially extended [Hara et al., 2007; Kanamori et al., 2013; Kobayashi et al., 2005; Shiraishi et al., 2005]. Other methods of distributed magnetic source imaging (dMSI) fit better the evidence that scalp IEDs arise from large sources [Engel, 1993; Merlet and Gotman, 1999; Schiller et al., 1998; Tao et al., 2007], as they assume the generator to be extended along the patient's cortical surface [Dale and Sereno, 1993]. Unlike ECD, dMSI is operator-independent, is robust to low signal to noise ratio and provides maps of cortical activations (see Tanaka and Stufflebeam [2013] for a review). In such context, the method entitled coherent Maximum Entropy on the Mean (cMEM) has been proposed and extensively evaluated by our group for its robustness and ability to recover the spatial extent of the IEDs generators along the cortical surface [Chowdhury et al., 2016; Grova et al., 2016; Heers et al., 2016; Pellegrino et al., 2016a]. Despite these positive properties, there is no evaluation of the clinical yield of dMSI.

We compared standard ECD to dMSI over a large dataset of MEG data from well-characterized epilepsy patients,

whose epileptic generator had been identified by invasive EEG (iEEG), surgery or a definite focal epileptogenic brain lesion. dMSI was performed with cMEM. Previous evidence suggests that similar spatial accuracy for the main peak of the generator could be achieved by minimum norm estimate (MNE) or standardized low-resolution electromagnetic tomography (sLORETA) [Chowdhury et al., 2013, 2016; Grova et al., 2016; Hedrich et al., 2017; Heers et al., 2016], whereas only cMEM could provide a localization sensitive to the underlying spatial extent of the generator and limited occurrence of distant, probably spurious, secondary sources [Heers et al., 2016].

## MATERIALS AND METHODS

### Patient Selection

This study complies with the Code of Ethics of the World Medical Association (Declaration of Helsinki). It was approved by the Montreal Neurological Institute Research Ethics Board and all patients signed a written informed consent prior to participation. Acquisitions were done at the Psychology Department of University of Montreal from 2006 to 2012 and at Montreal Neurological Institute McConnell Brain Imaging Center afterwards. We selected patients from our MEG database who fulfilled the inclusion criteria of a focal epilepsy with a well-defined epileptic focus. Exclusion criteria were <5 IEDs, magnetization artifact, and presence of extensive brain lesions (e.g., polymicrogyria).

### Definition of the Epileptic Focus

The ground truth definition of the epileptic focus was based on the combination of iEEG, epileptogenic MRI lesions, and cortex surgically resected [Pellegrino et al., 2016a; Pittau et al., 2014; Ryvlin et al., 2014]. For mesial temporal lobe patients, the epileptic focus included the lateral temporal regions and the mesial ones, to account for spikes depicted in scalp recordings as being generated in the temporal neocortex or propagated from mesial

generators [Koessler et al., 2015; Merlet and Gotman, 1999]. Before MEG analysis, the epileptic focus was manually drawn by two expert epileptologists (G.P. and E.K.) on each patient's MRI cortical surface.

### MEG Acquisitions and Preprocessing

Simultaneous MEG/EEG scans were performed in agreement with the American Clinical Magnetoencephalography Society (ACMEGS) guidelines [Bagic et al., 2011], using a CTF-MEG-system (MISL, Vancouver, Canada - 275 MEG gradiometers) with the patient lying down in a supine position. EEG analysis was not conducted for this study. Eye movements, heartbeat, and head position were continuously monitored with dedicated sensors. The sampling frequency was 600 Hz or higher (except for the first 3 patients scanned with a sampling frequency of 480 Hz). Acquisitions lasted about 1 h, divided in 6 min runs. Data preprocessing consisted of: third-order spatial gradient noise cancellation, DC removal, 60 Hz notch filter, band-pass filter [0.3–70 Hz], resampling to 600 Hz, visual identification of epileptic discharges, marking, and data segmentation (−1,000 ms to 1000 ms, 0 ms being the spike peak) [Heers et al., 2016; Pellegrino et al., 2016a,b]. MEG spikes were marked at their peak and grouped according to morphology and topography. Spikes belonging to the same group and run were averaged (at least five spikes) constituting a “study”. Each study, therefore, corresponded to an average of at least five IEDs of the same type and within the same run, was characterized by specific MEG time-course, MEG-MRI registration, and head model.

### MRI and Forward Model Estimation

The head model was built from each patient's high-resolution MRI (Siemens Tim Trio 3T scanner), using a T1W MPRAGE sequence with the following parameters: 1 mm isotropic 3D images, 192 sagittal slices,  $256 \times 256$  matrix, TE = 2.98 ms, TR = 2.3 s. The cortical mesh of the “mid” layer equidistant from the white/grey matter interface and the pial surface was reconstructed using the FreeSurfer toolbox [Dale et al., 1999]. Brainstorm software was used to reconstruct the inner skull surface, while coregistration between patient's MRI and functional MEG data was obtained through surface fitting between the anatomical head shape derived from the MRI and the head points digitized from the patient using a Polhemus localization system at the time of the acquisition [Tadel et al., 2011]. A single sphere head model was used for ECD, as indicated in the guidelines [Bagic et al., 2011], and a 1-layer boundary element method (BEM) using OpenMEEG method [Gramfort et al., 2010] was considered for dMSI. A comparison across multiple head models (single sphere, overlapping spheres, and BEM) was also performed.

### Source Localization Methods

Source localization was performed within a time window of 10 ms around the peak of the discharge. For ECD, single dipoles were fitted considering all MEG channels and without any a priori definition of the initialization point. A diagonal noise-covariance was modeled from a 1s baseline without any visually identified IEDs. dMSI methods, including cMEM, provide spatio-temporal maps of current density along the cortical surface at every time sample of interest. Among the multiple dMSI approaches available—LORETA, Minimum Norm Estimation (MNE) and many more [Tanaka and Stufflebeam, 2013]—we considered cMEM because (a) it has been specifically developed for the localization of IEDs; (b) it has the advantage of improving the contrast between the epileptic generator and surrounding regions, and (c) it is sensitive to the spatial extent of the generator along the cortical surface. cMEM is a probabilistic approach, offering an efficient framework to incorporate prior knowledge in the resolution of the source localization inverse problem [Amblard et al., 2004]. Brain activity is assumed to be organized by cortical parcels. A data-driven parcellation (DDP) method is used to cluster the whole cortical surface into  $K$  non-overlapping parcels [Lapalme et al., 2006], using partial information from the available data to guide this spatial clustering. The key aspect of DDP lies in the prelocalization of the sources of brain activity using the multivariate source prelocalization (MSP) method [Mattout et al., 2005], a projection method estimating, for each dipolar source, a coefficient, assessing its possible contribution to the data. DDP in  $K$  parcels is then obtained using a region-growing algorithm around the local maxima of the MSP map. In the MEM reference model, a hidden variable is associated to each parcel to model the probability of the parcel to be active or not (probability initialized using the MSP coefficients). In summary, using such a model, MEM provides an interesting framework allowing switching off the parcels that do not contribute to the solution, while preserving the ability to create a contrast of current intensities within the active parcels. In this study, we considered the coherent MEM method (cMEM), which further imposes a spatial smoothness constraint within each parcel. We have carefully evaluated the ability of cMEM to provide an accurate contrast along the spatial extent of the generator [Chowdhury et al., 2013, 2016; Grova et al., 2016; Hedrich et al., 2017; Heers et al., 2016]. The implementation of cMEM used in this study is available within the “Brain Entropy in space and time (BEst) plugin” in Brainstorm software (<http://neuroimage.usc.edu/brainstorm/Tutorials/TutBEst/>). The reader is referred to Chowdhury et al. [2013] for further methodological details.

### Measures of Performance and Statistical Analysis

We performed a study-based qualitative analysis based on the assessment of sublobar concordance with the focus,

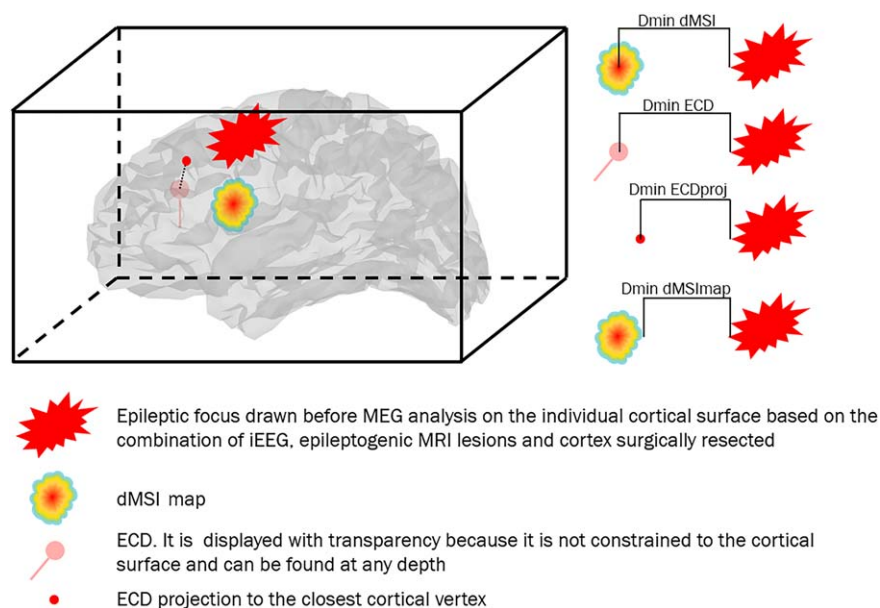


**Figure 1.**

Schematic representation of the quantitative performance measures under investigation. Dmin is the Euclidean distance expressed in mm between the source and the focus. The two main measures under investigation were (a) Dmin dMSI, which is the distance between the maximum intensity (one single vertex) of the cMEM cortical map and the closest point of the focus and (b) Dmin ECD, which is the distance between the ECD and the closest point of the focus. As ECD and dMSI are two very

and a quantitative measure of the distance of the generator from the epileptic focus (Fig. 1 and Supporting Information).

Sublobar concordance of ECD (or dMSI maximum) and the epileptic focus was defined on 20 sublobar regions [Pellegrino et al., 2016a]. We also performed a comparison restricted to the subgroup of cases corresponding to patients associated with a good postsurgical clinical outcome (Engel Class 1) [Engel Jr, 1993].

Quantitative analyses included (a) the minimum Euclidean distance (Dmin, expressed in mm) between the ECD (or dMSI map maximum) and the epileptic focus and (b) reproducibility based on the comparison of ECD and dMSI Dmin interquartile ranges of patients with multiple studies. Dmin provides a quantitative and reliable performance assessment, unbiased by the arbitrary selection of cortical regions [Pellegrino et al., 2016a]. In our analysis, we needed to take into account the intrinsic properties of the two methods which might bias the results toward a better performance of one or the other technique. As dMSI is localizing sources constrained along the cortical surface whereas ECD is not, and dMSI recovers a cortical region whereas ECD localizes only one point, we also considered the following additional comparisons for Dmin:

different methods, we also considered complementary measures: (a) Dmin ECDproj, which is the distance between the ECD projected to the closest cortical vertex and the closest point of the focus and (b) Dmin dMSImap, which is the distance between the border of cMEM cortical map thresholded at 30% and the closest point of the focus. [Color figure can be viewed at [wileyonlinelibrary.com](http://wileyonlinelibrary.com)]

- a. dMSI maximum versus ECD projection to the closest point of the cortical surface (ECDproj);
- b. dMSI map thresholded at 30% of its maximal amplitude [Heers et al., 2016] (dMSImap) versus ECD;
- c. dMSImap versus ECDproj.

The empirical level of 30% threshold for cMEM has been carefully tested in previous methodological and clinical investigations (Heers et al., 2014, 2016; Papadelis et al., 2016; Pellegrino et al., 2016a; von Ellenrieder et al., 2016). For this study, we also evaluated that, because of the excellent contrast provided by cMEM maps, a relatively large range of threshold values had limited impact on the size of the generator (See Supporting Information, and Supporting Information, Figs. 2 and 3 for further details). Indeed, cMEM provides maps with high contrast between the generator and surrounding regions, as also demonstrated by our previous studies [Chowdhury et al., 2013, 2015, 2016; Grova et al., 2006; Hedrich et al., 2017].

In addition to the study-based statistical analysis, a patient-based comparison of the two techniques was also performed for the two most relevant metrics, namely sublobar concordance and distance of the dipole/dMSI maximum from the epileptic focus. For patients with multiple

**TABLE I. Epidemiological and clinical features**

PA	Sex/age	EEG			SEEG			Surgery	Engel class
		IEDs	Ictal	Electrodes/side regions	Interictal	Ictal	MRI findings		
1	M/33	LP	LP						
2	F/28	LT	LT						LP FCD
3	M/35	LP	L FCP						L H atrophy with MTS L precuneus FCD
4	F/15	Bil F	Bil F						R F gyration abnormality
5	F/40	RT	RT						R H atrophy
6	F/27	RT	Bil T (R > L)						R H atrophy
7	M/42	LT	LT						LT atrophy and MTS
8	M/29	LT	LT						L H atrophy
9	F/27	L FT	L FT	5/L: A,Ha,Hp,Ca,OF	LF, LT	LF, LT			Sphenoethmoidal meningoencephalocele
10	M/15	Bil C	Bil C	3/R: RAC,SMA,Lesion	Lesion	Lesion			R F parasagittal FCD
11	F/58	RT	RT						R T atrophy
12	M/16	Bil FC (L > R)	Bil F	5/R:OF,Ca,Cm, SMAa,SMAP; 5/L: OF,Ca,Cm, SMAa,SMAP	bil F (L > R)	Bil F, max L SMA			L F
13	M/31	RT	RT						R T MTS
14	F/29	LT	LT						Signal abnormalities L A and the L subcortical T white matter.
15	F/19	RT	RT						R parahippocampal dysplasia
16	M/24	Bil F (L > R)	L F	4/R: OF,Ca,Cp,Lesion; 4/L: OF,Ca,Cp,F	Lesion, Bil F	Bil F, max Lesion			R parahippocampal resection L F FCD
17	F/34	RT	RT						R T atrophy and MTS
18	M/23	RT	RT						R T FCD
19	F/20	RF	RF						R F FCD
20	M/13	Bil T	Bil T (R > L)	4/R: A,H,Ca,OF; 5/L: A,H,OF,AC,SMA 9/R: OF,Ca,Cm,SMAa, SMAP,Ja,Ip,A; 1/L:Hc	L H	L H			H malrotation
21	M/32	Bil F (R > L)	RF	9/R: OF,Ca,Cm,SMAa, SMAP,Ja,Ip,A; 1/L:Hc	R OF,Ja	R OF,Ja			R hemimegalencephally
22	M/32	R FT	RF	9/R: A,H,Ja,Ip,OF,Ca, Cm,SMAa,SMAP	OF,Ja,A,H	OF, Ja, Operculum			R OF
23	F/25	R FT	RF	9/R: A,Ha,Hp,Im,OF,Ca, Cm,SMAa,SMAP	OF, F convexity, Ta neocortex	OF			R OF
24	M/20	L CP	L CP	8x8 GRID L FCT convexity	Rolandic m	Sensory P			L post C
25	M/41	R FC	R FC	9/R: A,Ha,Hp,Ip,OF, SMA,Ca,Cp,P	H,SMA,Cm,OF	T,SMA			R F
26	M/23	RT	RT						R T atrophy
27	F/39	RT	RT						R MTS
28	M/32	RT	RT						R MTS



TABLE 1. (continued).

P/A	Sex/age	EEG			SEEG			Surgery	Engel class	
		IEDs	Ictal	Electrodes/side regions	Interictal	Ictal	MRI findings			
29	F/19	LT	LT							
30	F/22	RF	RF	2/L: H,Ip; 7/R: H,Ip,SMAa,SMAM,SMAP,Ca,Cp	R SMAa,SMAM,SMAP	R SMA		L T (superior gyrus, posterior) FCD R F FCD	RF	3
31	M/19	RT	RT							
32	F/24	Bil F	Bil F (R > L)	7/R: H,OF,Fp,Ca,Cm, SMAa,SMAP; 2/L:OF,Ca	Bil F (R > L);	Bil F (R > L)		R H atrophy and MTS R F FCD	R AH	1
33	M/25	LT	LT							
34	M/39	RC	R FC	2/L: SMAa,SMAP; 6/R: H,I,Ca,Cp,SMAa,SMAP	R SMAP	R SMAP		L MTS, L A DNET R FC parasagittal FCD	R A	
35	M/39	R C	R FC	2/L: SMAa,SMAP; 6/R: H,I,Ca,Cp,SMAa,SMAP	R SMAP, R CP	R SMAP		R FC parasagittal FCD		
36	M/34	Bil FC	R FC	7/R: A,H,OF,Ca,Cm,Ia,Ip	Fm	Fm		R Fm FCD	R Fm	1
37	M/38	R FT	R FT	8/R: Fa,OF,Ca,Cp, SMAa,SMAP,A,H	OF	OF		R OF FCD	R OF	1
38	F/38	L FT	L FT	5/L: A,Ha,Hp,Ca,OF	T neocortical and mesial	T neocortical and mesial		L H malrotation	L AH	4
39	M/29	L FC	L FC							
40	M/33	Bil T	Bil T (L>R)	4/L: A,Ha,Hp,Fusiform; 4/R: A,Ha,Hp,Fusiform	Bil A, T and Hc	L and R T		R F polar FCD L H atrophy	R F polar	1
41	M/35	LT	L FT	2/R: Ca, Ha; 9/L: A,Ha, Hp,OF,Ia,Fa,Ca,SMAa,SMAP	L I, FO, T	FO		L OF FCD	L F	
42	M/55	RT	RT							
43	F/22	L FT	L FCT	7/L:OF,G. Rectus,Ca, Cp,LA,Ha,Hp	L Ca, T pole, Hp, A	L Ca Ta		R T atrophy and MTS L Ca, OF FCD	R Ta L Ta, OF	1 1
44	M/37	Bil FT	R FT	7/L: OF,Ca, Ca,Cm,Cp, Ha,Hp; 2/R: Ha,OF	Bil Ha, Hp	Bil T		Bil H Atrophy		
45	F/19	L FT	L FT							
46	F/22	L P	-							
47	F/30	L FC	L F							
48	F/28	Bil F (L>R)	L F							
49	M/60	RT	RT							

L = left; R = right; Bil = bilateral; F = frontal; C = central; P = parietal; O = occipital; A = anterior; m = middle; p = posterior; Post Quad = posterior quadrant; SMA = supplementary motor area; C = cingulate; H = hippocampus; A = amigdala; I = insula; OF = orbito frontal; FCD = focal cortical dysplasia; MTS = mesial temporal sclerosis; AH = amygdalohippocampotomy.

**TABLE II. Summary of results**

		ECD	cMEM	Test value, <i>P</i> value	
<b>Sublobar concordance</b>	All	235/340 (69%)	277/340 (81%)	$\chi^2 = 19.547, P < 0.001^a$	
	Extratemporal	137/206 (67%)	174/206 (84%)	$\chi^2 = 25.412, P < 0.001^a$	
	Temporal	98/134 (73%)	103/134 (77%)	$\chi^2 = 0.457, n.s.$	
	Engel Class 1	67/96 (70%)	80/96 (83%)	$\chi^2 = 9.600, P = 0.001$	
<b>Dmin</b>	dMSI vs ECD	All	4.88 (64.65)	3.44 (76.01)	$z = -4.827, P < 0.001^b$
		Temporal	3.73 (60.33)	0.00 (63.69)	$z = -2.332, P = 0.020^b$
		Extratemporal	5.54 (64.54)	4.92 (76.01)	$z = -4.250, P < 0.001^b$
	dMSI vs ECDproj	All	0 (67.20)	3.44 (76.01)	$z = 5.896, P < 0.001^b$
	dMSImap vs ECD	All	4.88 (64.65)	0 (79.49)	$z = -15.673, P < 0.001^b$
	dMSImap vs ECDproj	All	0 (67.20)	0 (79.49)	$z = -6.590, P < 0.001^b$

<sup>a</sup>McNemar's test.

<sup>b</sup>Wilcoxon Signed-Rank Test.

n.s. = not significant.

Dmin = minimum Euclidean distance expressed in mm and reported as median (range); dMSI = distributed magnetic source imaging considering the point with the highest source amplitude (maximum); ECD = equivalent current dipole; ECDproj = ECD projection to the closest cortical point; dMSImap = dMSI map thresholded at 30% of its maximal amplitude; All = all studies; Extratemporal = non temporal lobe epilepsy patients; Temporal = temporal lobe epilepsy patients.

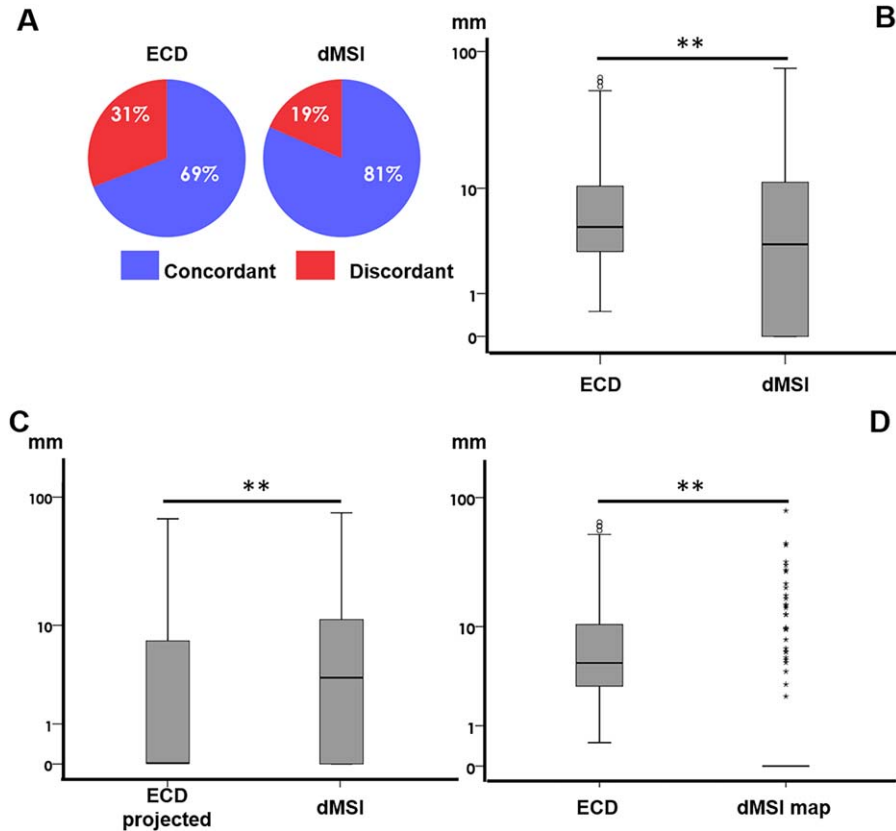


**Figure 2.**

Source localization in comparison with the epileptic focus. Panel A. Concordance at sublobar level versus epileptic focus. Panel B. Boxplot distribution of Dmin comparing ECD and dMSI. The minimum distance was significantly lower for dMSI. The median difference between dMSI and ECD was in the range of few millimeters. The median Dmin of the dipole projection to the closest cortical point was significantly

lower than dMSI Dmin (Panel C). However, when taking into account that dMSI recovers a cortical region (cMEM map thresholded at 30% of its maximum amplitude, Dmin became significantly smaller (Panel D). Note that Dmin values along the y axis are in logarithmic scale. [Color figure can be viewed at [wileyonlinelibrary.com](http://wileyonlinelibrary.com)]

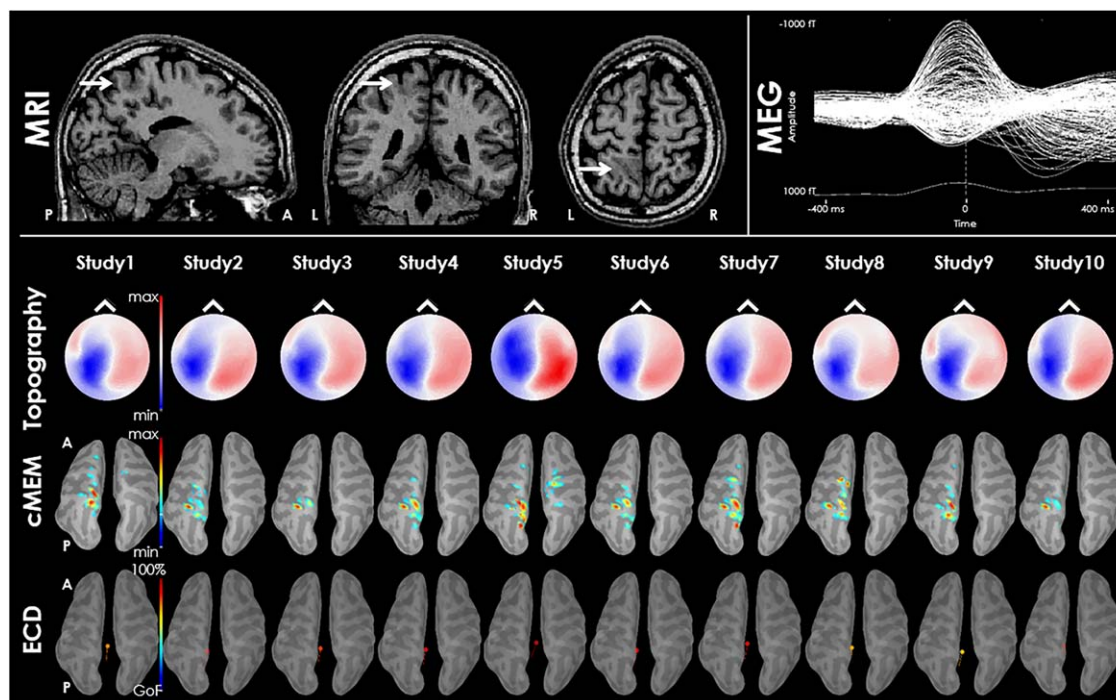


**Figure 3.**

Refractory epilepsy related to focal cortical dysplasia of the left parietal cortex. Top left panel: MRI shows a focal cortical dysplasia (arrow). Top right panel: MEG signal of the average IED for one study. Lower panel: comparison between ECD and dMSI. For all the studies, the first line shows the topography of MEG signal, the second line shows the cMEM source localization, and the third line shows the ECD source localization. dMSI accurately localizes the generator for all the studies, which is concordant with the anatomical lesion and provides an estimation

of the spatial extent of the generator. ECD shows a good performance; however, the dipole is sometimes shifted toward the midline (especially for the studies 1 and 5). The cortical surface of the source localization pictures has been inflated and is shown with transparency for ECD to allow the visualization of deep dipoles. dMSI maps have been thresholded at 30% of the local maximum. GoF = goodness of fit. [Color figure can be viewed at [wileyonlinelibrary.com](http://wileyonlinelibrary.com)]

studies, sublobar concordance was defined when concordant studies occurred more than discordant ones, and Dmin was computed as median Dmin across studies.

McNemar's tests were used to assess differences of sublobar concordance. Wilcoxon Signed-Rank tests were used to assess Dmin and interquartile range differences. Significance levels were set at  $P < 0.05$ .

## RESULTS

A total of 340 studies from 49 patients (age  $29.98 \pm 10.48$  years, 28M–21F, median studies per patient = 6) were analyzed, 134 of which were from mesial temporal lobe patients. Clinical details are reported in Table I. The ground truth definition of the epileptic focus was based on: MRI lesion alone (12 patients), iEEG + MRI lesion (6), iEEG + Surgery (3), MRI lesion + Surgery (16), MRI lesion + iEEG + Surgery (12). The size of the focus delineated manually along the cortical surface ranged from

33.85 to 461.78 cm<sup>2</sup>, with a median size of 80.51 cm<sup>2</sup>. A reliable follow-up was available for 25 patients (extratemporal = 17, temporal = 8), corresponding to 167 source localizations for which surgical outcome were distributed as follows: Engel 1 = 96, Engel 2 = 11, Engel 3 = 27, and Engel 4 = 33 (Table I). Engel Class 1 outcome corresponds to a very good clinical outcome, with patients free of disabling seizures, whereas Engel Class 4 outcome corresponds to a poor outcome with patients showing no worthwhile clinical improvement. Engel Class 1 outcome is usually achieved when the generator of epileptic seizures is fully resected [Engel Jr, 1993].

### Sublobar Concordance

Sublobar concordance with the epileptic focus was significantly higher for dMSI when compared to ECD (235/340 (69%), 277/340 (81%), McNemar's  $\chi^2 = 19.547$ ,  $P < 0.001$ ) (Table II and Figs. 2A and 3–6). dMSI concordance was higher for both temporal and extratemporal



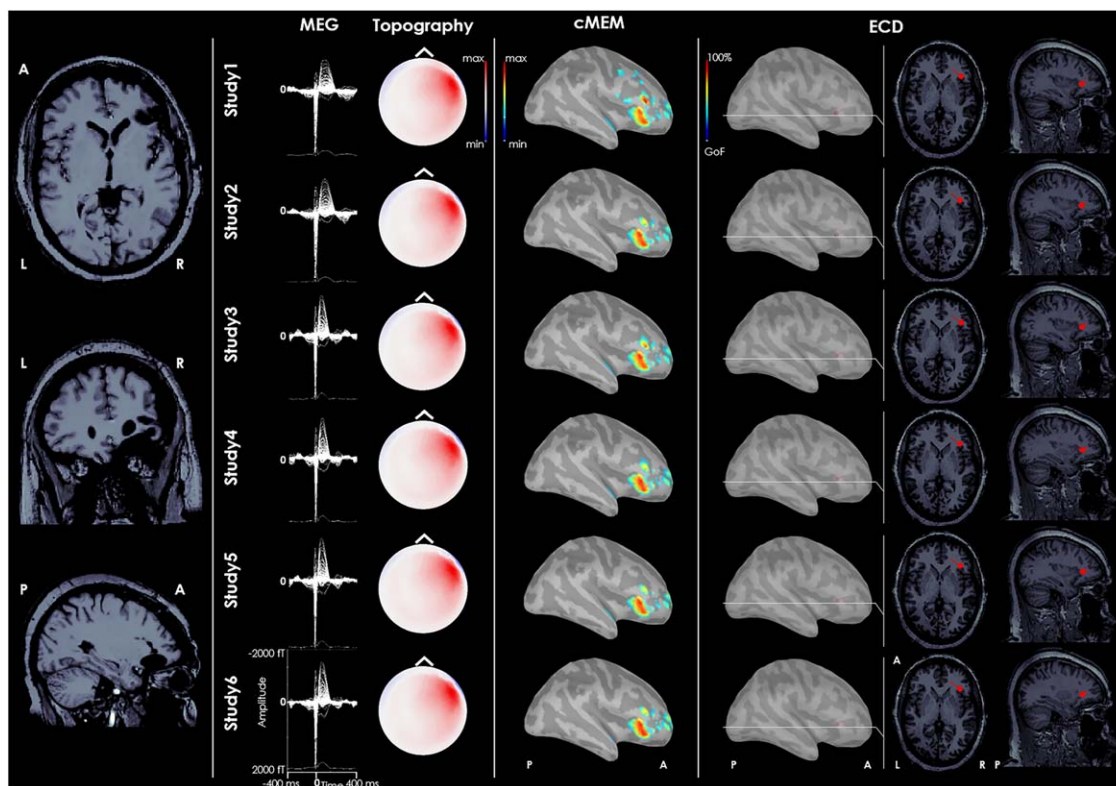


**Figure 4.**

Refractory epilepsy related to focal cortical dysplasia of the right frontal operculum. From left to right: postsurgical MRI, MEG signal of the average IED for each study, topography of MEG signal, dMSI source imaging, and ECD source localization. MEG signals were highly reproducible. The generator recovered by dMSI is concordant with the epileptic focus and provides an estimate of

its extent. ECD source localization is concordant with the focus and very consistent as well. The dipole was however quite deep, close to the insula. It is almost impossible to appreciate it through the cortical surface and it has been displayed over brain sections in right last columns. [Color figure can be viewed at [wileyonlinelibrary.com](http://wileyonlinelibrary.com)]

lobe studies (McNemar's  $\chi^2 = 17.96$ ,  $P < 0.001$ ) (Table II, Fig. 6, and Supporting Information, Fig. 6), even though no statistically significant difference was found for temporal lobe. Out of 98 concordant temporal ECD sources, 44 were localized deep within the temporal lobe (11 in the subcortical white matter and 33 deeper in more mesial structures) (Fig. 5 and Supporting Information, Fig. 6). As epileptic activity generated within the mesial part of the temporal lobe cannot be recorded with sufficient amplitude to be seen from scalp recordings [Koessler et al., 2015; Merlet and Gotman, 1999], these results may appear methodologically inconsistent and incongruent with the clinical hypothesis. When excluding mesial temporal regions from the focus, ECD sublobar concordance drops from 235/340 (69%) to 191/340 (56%). The comparison restricted to the cases with a good post-surgical outcome (i.e., seizure freedom, Engel Class 1) showed significantly higher sublobar concordance for dMSI than ECD (McNemar's  $\chi^2 = 9.600$ ,  $P = 0.001$ ). Finally, when considering a patient-based analysis, dMSI showed a significantly higher

sublobar concordance than ECD (42/49 (86%) vs 34/49 (69%), McNemar's  $\chi^2 = 4.900$ ,  $P = 0.021$ ) (Fig. 7 Panel A).

### Distance and Reproducibility

The median distance between the dipole and the epileptic focus (Dmin) over all source localizations considered was smaller than 5 mm for both methods (4.88 mm for ECD and 3.44 mm for dMSI; Table II). dMSI was significantly better than ECD, but the effect size was small (1–2 mm difference of the median) (Wilcoxon Signed-Rank Test,  $z = -4.827$ ,  $P < 0.001$ ) (Table II and Fig. 2B). These results were similar for temporal and extratemporal studies (Table II). These results were confirmed when considering a patient-based analysis, with dMSI finding the generator closer to the epileptic focus than ECD (Wilcoxon Signed-Rank Test  $z = -2.044$ ,  $P = 0.041$ ) (Fig. 7 Panel B).

Reproducibility between studies for each patient showed no significant differences in interquartile ranges of Dmin

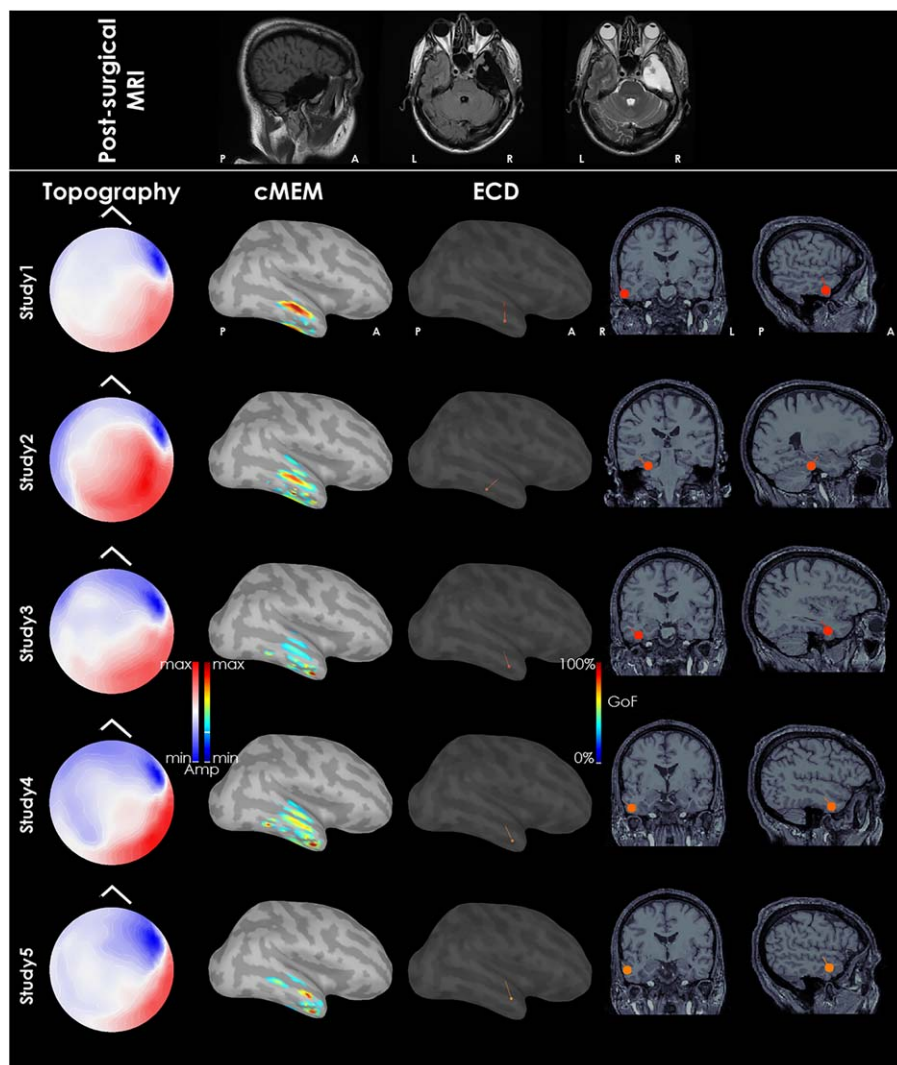


**Figure 5.**

Patient affected by drug-resistant temporal lobe epilepsy. Upper panel shows the postsurgical MRI. dMSI localizes the generator in the lateral temporal cortex. ECD dipoles are localized in the temporal lobe at different depth from run to run. In two cases (Study 2 and Study 3), the dipole is localized in the mesial temporal structures. [Color figure can be viewed at [wileyonlinelibrary.com](http://wileyonlinelibrary.com)]

between dMSI and ECD (Wilcoxon Signed-Rank test,  $P > 0.200$ ).

### Properties of the Two Methods

After projecting every ECD to the closest vertex on the cortical surface (median (range) distance = 3.51 (35.80) mm), ECD-projected Dmin became significantly lower than dMSI Dmin ( $z = -5.896$ ,  $P < 0.001$ ) (Fig. 2C). However, dMSI was providing better performance than ECD when taking into account the spatial extent of the generators (Figs. 2D, 3, and 4). Indeed, when considering cMEM maps thresholded at 30% of their maximum value, Dmin dMSI was significantly lower than both Dmin ECD

( $z = -15.673$ ,  $P < 0.001$ ) and Dmin ECD projected to the closest cortical point ( $z = -6.590$ ,  $P < 0.001$ ) (Fig. 2D).

Finally, we observed that at the level of our proposed quantitative evaluation, the choice of the head model had no significant impact on both Dmin ECD and Dmin dMSI (single sphere vs overlapping spheres for ECD and overlapping spheres vs BEM for dMSI, Mann-Whitney test,  $P > 0.200$  consistently) (Supporting Information, Fig. 4).

### DISCUSSION AND CONCLUSION

Our systematic validation of the performance of dMSI using cMEM in comparison with the clinically approved

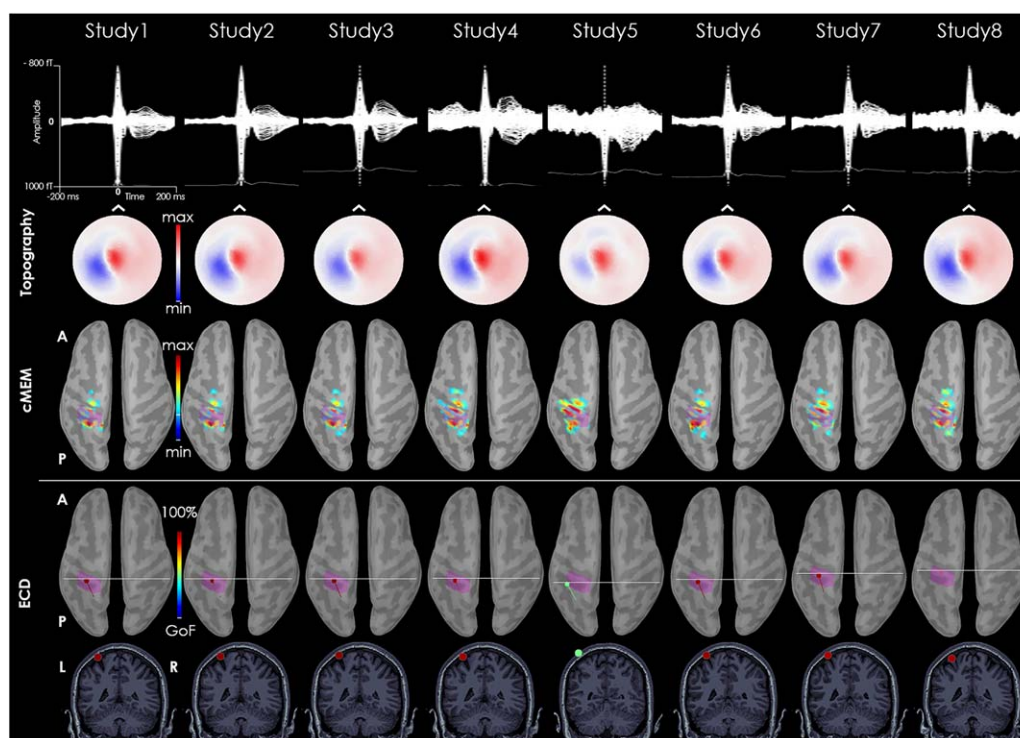


**Figure 6.**

Patients with focal cortical dysplasia in the left postcentral gyrus. The MEG signal of the average IEDs time-course is pretty consistent across studies. MEG topography at the peak is also very stable across studies. Whereas dMSI always recovers the interictal source with an estimation of its extent in the left postcentral

gyrus, ECD localization corresponds to the same area, but the dipole is very close to the skull or even outside it. The pink cortex corresponds to the epileptic focus as assessed by iEEG. [Color figure can be viewed at [wileyonlinelibrary.com](http://wileyonlinelibrary.com)]

ECD showed that both methods localize the IEDs generator very close to the epileptic focus, with dMSI providing significantly better performance. The difference in sublobar concordance suggested that ECD exhibited more often distant failure when compared to dMSI (31% vs 19%, Fig. 1A). Such difference is clinically relevant particularly when focusing on the source localizations in those patients who had undergone a complete resection of the epileptic focus and became seizure-free after surgery (Engel Class 1) (83% vs 70% sublobar concordance).

Our cohort included patients with extratemporal and mesial temporal epilepsy. Those with mesial temporal epilepsy are not ideal candidates for MEG, as the epileptic focus can be well defined with video-EEG monitoring, neuropsychology evaluation, and high-resolution MRI [Moshé et al., 2015; Ryvlin et al., 2014]. However, also for these cases, dMSI outperformed ECD, possibly because of its ability to model spatially extended generators [von Ellenrieder et al., 2016]. In our experience ECD could be found at any depth in the temporal lobe, up to the mesial temporal structures (Fig. 5, Supporting Information, Fig. 6), but epileptic activity confined to deep regions cannot generate signals of sufficient large amplitude to be

detected on the scalp, and detected signals more likely result from propagated activities [Koessler et al., 2015; Merlet and Gotman, 1999]. When excluding the mesio-temporal structures from the presumed generator, ECD sublobar concordance would drop from 69% to 56%. Deep dipoles often correspond to large generators located in the lateral and polar temporal neocortex. Their interpretation requires special attention as there is no unambiguous way to disentangle deep dipoles related to deep generators from apparent deep dipoles but mislocalized because of spatially extended sources [Ebersole and Ebersole, 2010; Gloor, 1985].

The study of Dmin, a measure of absolute distance insensitive to the criteria to define sublobar regions, confirmed the overall superiority of dMSI using cMEM and also highlighted that the median difference between the two techniques was only a few millimeters. Dmin might not be the most appropriate metric to evaluate the performance of ECD, as the latter requires some degree of interpretation to figure out the generator linked to the dipole. Indeed, the combination of the dipole location and its orientation are two important parameters to be considered for clinical interpretation. In this respect, for quantitative



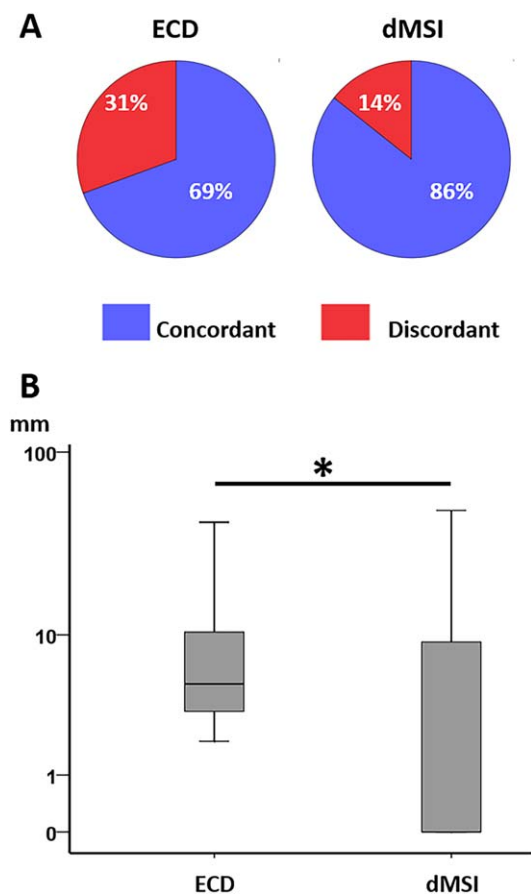


**Figure 7.**

Patient level analysis. Panel A: concordance at sublobar level versus epileptic focus ECD on the left, dMSI on the right. Panel B: boxplot distribution of  $D_{min}$  comparing ECD and dMSI. The minimum distance was significantly lower for dMSI. The median difference between dMSI and ECD was in the range of few millimeters. [Color figure can be viewed at [wileyonlinelibrary.com](http://wileyonlinelibrary.com)]

evaluation purposes, we added the study of the distance from the focus of the ECD projection on the cortical surface and showed a significantly better performance of ECD projection when compared to dMSI maximum, but again the median difference was just a few millimeters. However, when taking into account the extent of the generator estimated by dMSI (dMSI map), the median  $D_{min}$  dropped to 0 mm, suggesting that most often dMSI generators spatially overlapped with the epileptic focus, therefore performing far better than ECD. Finally, both methods showed a comparable degree of within subject reproducibility (Fig. 4 and Supporting Information, Fig. 5). Comparable results were also confirmed at patient level analysis (Fig. 7). In this respect, two very different methods give approximately the same result and converge to provide a useful clinical solution.

As opposed to point-sources localized with ECD, dMSI has the definite advantage of estimating the spatial extent

of the generator (Figs. 2, 3, and 5). This feature, which has been carefully validated with dedicated iEEG-MEG studies for the cMEM algorithm used in this study [Grova et al., 2016], can assist the clinician in cases where cortex needs to be targeted for invasive EEG electrodes positioning or for surgical resection, and can be exploited for neuronavigation purposes. A systematic comparison of multiple dMSI approaches was beyond the scope of this investigation. As already pointed out, previous evidence suggests that similar spatial accuracy for the main peak of the generator could be achieved by minimum norm estimate (MNE) or standardized low-resolution electromagnetic tomography (sLORETA), while only cMEM would accurately provide an estimate of the underlying spatial extent [Chowdhury et al., 2013, 2016; Grova et al., 2016; Hedrich et al., 2017; Heers et al., 2016]. To be noted that the estimation of the spatial extent of the generator for cMEM has been performed relying on an empirical 30% threshold of the cortical map. This strategy is specific for cMEM and has been previously tested in both methodological and clinical contexts [Hedrich et al., 2017; Heers et al., 2014, 2016; Papadelis et al., 2016; Pellegrino et al., 2016a; von Ellenrieder et al., 2016], whereas the excellent contrast provided by cMEM maps allows the choice of such a threshold to be less critical (Supporting Information, Figs. 2 and 3). Other inverse solutions able to provide an estimation of the spatial extent need specific approaches [Becker et al., 2014, 2017; Jung et al., 2013; Sohrabpour et al., 2016; Zhu et al., 2014]. Finally, caution should be considered when generalizing our results to all epilepsy surgical candidates evaluated with MEG, especially for those with large cortical lesions. We excluded from this study patients with a very extended lesion because of the difficulty of computing an accurate head model in such cases.

An additional advantage of using dMSI is that this technique is largely operator-independent. On the contrary, ECD is operator-dependent and often requires (a) a-priori definition of the number of dipoles to fit, (b) selection of the brain region for initializing the dipole position, (c) selection of a subsample of MEG channels for modeling multiple parts of complex sources, and (d) manual identification of a narrow time-window of interest [Bagic et al., 2011; Ebersole and Ebersole, 2010].

The widespread use of a source localization method is very dependent on the availability of reliable and user-friendly software for daily use. This has largely favored ECD during the last 30 years, as dipole fitting toolboxes are included in the MEG scanner software [Hamandi et al., 2016]. This barrier has been recently overcome by several reliable and free toolboxes—Brainstorm [Tadel et al., 2011], MNE [Gramfort et al., 2014; Tanaka and Stufflebeam, 2013], and fieldtrip [Oostenveld et al., 2011]—allowing distributed source imaging with a very user-friendly approach.

A recent European survey [Mouthaan et al., 2016] reveals that tertiary epilepsy centers already use

distributed electromagnetic source localization procedures in the presurgical workup of epilepsy patients. Our study conducted on a large sample size of patients with epilepsy, guarantees more confidence in these methods and enhances awareness about their potential and limitations. As for every source imaging technique, dMSI requires proper clinical judgment and interpretation of the results in the light of the entire clinical framework [Bagić, 2016]. As dMSI using cMEM provides robust and reproducible results and offers the advantage of being sensitive to the spatial extent of the generator to be targeted for invasive EEG or removed during epilepsy surgery, it should complement — or even replace — ECD in daily clinical practice.

### ACKNOWLEDGMENT

The authors thank professor J. Gotman from the Montreal Neurological Institute for fruitful discussions and manuscript revision.

### REFERENCES

- Amblard C, Lalpalme E, Lina JM (2004): Biomagnetic source detection by maximum entropy and graphical models. *IEEE Trans Biomed Eng* 51:427–442.
- Bagić A (2016): Look back to leap forward: The emerging new role of magnetoencephalography (MEG) in nonlesional epilepsy. *Clin Neurophysiol* 127:60–66.
- Bagić AI, Knowlton RC, Rose DF, Ebersole JS, Committee ACPG (2011): American clinical magnetoencephalography society clinical practice guideline 1: Recording and analysis of spontaneous cerebral activity\*. *J Clin Neurophysiol* 28:348–354.
- Barth DS, Sutherling W, Engel J, Beatty J (1982): Neuromagnetic localization of epileptiform spike activity in the human brain. *Science* 218:891–894.
- Bast T, Oezkan O, Rona S, Stippich C, Seitz A, Rupp A, Fauser S, Zentner J, Rating D, Scherg M (2004): EEG and MEG source analysis of single and averaged interictal spikes reveals intrinsic epileptogenicity in focal cortical dysplasia. *Epilepsia* 45: 621–631.
- Becker H, Albera L, Comon P, Haardt M, Birot G, Wendling F, Gavaret M, Bénar C-G, Merlet I (2014): EEG extended source localization: Tensor-based vs. conventional methods. *NeuroImage* 96:143–157.
- Becker H, Albera L, Comon P, Nunes J-C, Gribonval R, Fleureau J, Guillotel P, Merlet I (2017): Sissy: An efficient and automatic algorithm for the analysis of EEG sources based on structured sparsity. *NeuroImage*
- Chowdhury R, Merlet I, Birot G, Kobayashi E, Nica A, Biraben A, Wendling F, Lina J, Albera L, Grova C (2016): Complex patterns of spatially extended generators of epileptic activity: Comparison of source localization methods cMEM and 4-ExSoMUSIC on High Resolution EEG and MEG data. *NeuroImage*
- Chowdhury RA, Lina JM, Kobayashi E, Grova C (2013): MEG source localization of spatially extended generators of epileptic activity: Comparing entropic and hierarchical bayesian approaches. *PLoS One* 8:e55969.
- Chowdhury RA, Zerouali Y, Hedrich T, Heers M, Kobayashi E, Lina JM, Grova C (2015): MEG-EEG information fusion and electromagnetic source imaging: From theory to clinical application in epilepsy. *Brain Topogr.*
- Dale AM, Fischl B, Sereno MI (1999): Cortical surface-based analysis: I. Segmentation and surface reconstruction. *NeuroImage* 9: 179–194.
- Dale AM, Sereno MI (1993): Improved localization of cortical activity by combining EEG and MEG with MRI cortical surface reconstruction: A linear approach. *J Cogn Neurosci* 5:162–176.
- Darvas F, Pantazis D, Kucukaltun-Yildirim E, Leahy RM (2004): Mapping human brain function with MEG and EEG: Methods and validation. *NeuroImage* 23 Suppl 1:S289–S299.
- Ebersole JS, Ebersole SM (2010): Combining MEG and EEG source modeling in epilepsy evaluations. *J Clin Neurophysiol* 27: 360–371.
- Engel J Jr (1993): Intracerebral recordings: Organization of the human epileptogenic region. *J Clin Neurophysiol* 10:90–98.
- Engel Jr, J (1993): Outcome with respect to epileptic seizures. Surgical treatment of the epilepsies: 609–621.
- Gloor P (1985): Neuronal generators and the problem of localization in electroencephalography: Application of volume conductor theory to electroencephalography. *J Clin Neurophysiol* 2: 327–354.
- Gramfort A, Luessi M, Larson E, Engemann DA, Strohmeier D, Brodbeck C, Parkkonen L, Hämäläinen MS (2014): MNE software for processing MEG and EEG data. *NeuroImage* 86:446–460.
- Gramfort A, Papadopoulos T, Olivi E, Clerc M (2010): OpenMEEG: Opensource software for quasistatic bioelectromagnetics. *Biomed Eng Online* 9:45.
- Grova C, Aiguabella M, Zelmann R, Lina JM, Hall JA, Kobayashi E (2016): Intracranial EEG potentials estimated from MEG sources: A new approach to correlate MEG and iEEG data in epilepsy. *Hum Brain Mapp.*
- Grova C, Daunizeau J, Lina JM, Benar CG, Benali H, Gotman J (2006): Evaluation of EEG localization methods using realistic simulations of interictal spikes. *NeuroImage* 29:734–753.
- Hamandi K, Routley BC, Koelewijn L, Singh KD (2016): Non-invasive brain mapping in epilepsy: Applications from magnetoencephalography. *J Neurosci Methods* 260:283–291.
- Hara K, Lin F-H, Camposano S, Foxe D, Grant P, Bourgeois B, Ahlfors S, Stufflebeam S (2007): Magnetoencephalographic mapping of interictal spike propagation: A technical and clinical report. *Am J Neuroradiol* 28:1486–1488.
- Hedrich T, Pellegrino G, Kobayashi E, Lina J, Grova C (2017): Comparison of the spatial resolution of source imaging techniques in high-density EEG and MEG. *NeuroImage*
- Heers M, Chowdhury RA, Hedrich T, Dubeau F, Hall JA, Lina J-M, Grova C, Kobayashi E (2016): Localization accuracy of distributed inverse solutions for electric and magnetic source imaging of interictal epileptic discharges in patients with focal epilepsy. *Brain Topogr* 29:162–181.
- Heers M, Hedrich T, An D, Dubeau F, Gotman J, Grova C, Kobayashi E (2014): Spatial correlation of hemodynamic changes related to interictal epileptic discharges with electric and magnetic source imaging. *Hum Brain Mapp* 35:4396–4414.
- Jung J, Bouet R, Delpuech C, Ryvlin P, Isnard J, Guenot M, Bertrand O, Hammers A, Mauguière F (2013): The value of magnetoencephalography for seizure-onset zone localization in magnetic resonance imaging-negative partial epilepsy. *Brain* 136:3176–3186.
- Kanamori Y, Shigeto H, Hironaga N, Hagiwara K, Uehara T, Chatani H, Sakata A, Hashiguchi K, Morioka T, Tobimatsu S (2013): Minimum norm estimates in MEG can delineate the



- onset of interictal epileptic discharges: A comparison with ECoG findings. *NeuroImage Clin* 2:663–669.
- Knowlton R, Laxer K, Aminoff M, Roberts T, Wong S, Rowley H (1997): Magnetoencephalography in partial epilepsy: Clinical yield and localization accuracy. *Ann Neurol* 42:622–631.
- Knowlton RC, Elgavish R, Howell J, Blount J, Burneo JG, Faught E, Kankirawatana P, Riley K, Morawetz R, Worthington J, Kuzniecky RI (2006): Magnetic source imaging versus intracranial electroencephalogram in epilepsy surgery: A prospective study. *Ann Neurol* 59:835–842.
- Kobayashi K, Yoshinaga H, Ohtsuka Y, Gotman J (2005): Dipole modeling of epileptic spikes can be accurate or misleading. *Epilepsia* 46:397–408.
- Koessler L, Cecchin T, Colnat-Coulbois S, Vignal J-P, Jonas J, Vespignani H, Ramantani G, Maillard LG (2015): Catching the invisible: Mesial temporal source contribution to simultaneous EEG and SEEG recordings. *Brain Topogr* 28:5–20.
- Lapalme E, Lina J-M, Mattout J (2006): Data-driven parceling and entropic inference in MEG. *NeuroImage* 30:160–171.
- Mattout J, Pélérini-Issac M, Garnero L, Benali H (2005): Multivariate source prelocalization (MSP): Use of functionally informed basis functions for better conditioning the MEG inverse problem. *NeuroImage* 26:356–373.
- Merlet I, Gotman J (1999): Reliability of dipole models of epileptic spikes. *Clin Neurophysiol* 110:1013–1028.
- Moshé SL, Perucca E, Ryvlin P, Tomson T (2015): Epilepsy: New advances. *Lancet* 385:884–898.
- Mouthaan BE, Rados M, Barsi P, Boon P, Carmichael DW, Carrette E, Craiu D, Cross JH, Diehl B, Dimova P (2016): Current use of imaging and electromagnetic source localization procedures in epilepsy surgery centers across Europe. *Epilepsia*
- Oostenveld R, Fries P, Maris E, Schoffelen J-M (2011): FieldTrip: Open source software for advanced analysis of MEG, EEG, and invasive electrophysiological data. *Comput Intell Neurosci* 2011:1.
- Papadelis C, Tamilya E, Stufflebeam S, Grant PE, Madsen JR, Pearl PL, Tanaka N (2016): Interictal high frequency oscillations detected with simultaneous magnetoencephalography and electroencephalography as biomarker of pediatric epilepsy. *J Vis Exp JoVE*.
- Pellegrino G, Hedrich T, Chowdhury R, Hall JA, Lina JM, Dubeau F, Kobayashi E, Grova C (2016a): Source localization of the seizure onset zone from ictal EEG/MEG data. *Hum Brain Mapp*.
- Pellegrino G, Machado A, von Ellenrieder N, Watanabe S, Hall JA, Lina J-M, Kobayashi E, Grova C (2016b): Hemodynamic response to interictal epileptiform discharges addressed by personalized EEG-fNIRS recordings. *Front Neurosci* 10:102.
- Pittau F, Grouiller F, Spinelli L, Seeck M, Michel CM, Vuillmoz S (2014): The role of functional neuroimaging in pre-surgical epilepsy evaluation. *Front Neurol* 5:31.
- Ryvlin P, Cross JH, Rheims S (2014): Epilepsy surgery in children and adults. *Lancet Neurol* 13:1114–1126.
- Scherg M, Von Cramon D (1985): Two bilateral sources of the late AEP as identified by a spatio-temporal dipole model. *Electroencephalogr Clin Neurophysiol Evoked Potent Sect* 62: 32–44.
- Schiller Y, Cascino GD, Sharbrough FW (1998): Chronic intracranial EEG monitoring for localizing the epileptogenic zone: An electroclinical correlation. *Epilepsia* 39:1302–1308.
- Shiraishi H, Ahlfors SP, Stufflebeam SM, Takano K, Okajima M, Knake S, Hatanaka K, Kohsaka S, Saitoh S, Dale AM (2005): Application of magnetoencephalography in epilepsy patients with widespread spike or slow-wave activity. *Epilepsia* 46: 1264–1272.
- Sohrabpour A, Lu Y, Worrell G, He B (2016): Imaging brain source extent from EEG/MEG by means of an iteratively reweighted edge sparsity minimization (ires) strategy. *NeuroImage* 142:27–42.
- Stefan H, Hummel C, Scheler G, Genow A, Druschky K, Tilz C, Kaltenhauser M, Hopfengartner R, Buchfelder M, Romstock J (2003): Magnetic brain source imaging of focal epileptic activity: A synopsis of 455 cases. *Brain* 126:2396–2405.
- Tadel F, Baillet S, Mosher JC, Pantazis D, Leahy RM (2011): Brainstorm: A user-friendly application for MEG/EEG analysis. *Comput Intell Neurosci* 2011:879716.
- Tanaka N, Stufflebeam SM (2013): Clinical application of spatio-temporal distributed source analysis in presurgical evaluation of epilepsy. *Front Hum Neurosci* 8:62–62.
- Tao JX, Baldwin M, Hawes-Ebersole S, Ebersole JS (2007): Cortical substrates of scalp EEG epileptiform discharges. *J Clin Neurophysiol* 24:96–100.
- von Ellenrieder N, Pellegrino G, Hedrich T, Gotman J, Lina J-M, Grova C, Kobayashi E (2016): Detection and magnetic source imaging of fast oscillations (40–160 Hz) recorded with magnetoencephalography in focal epilepsy patients. *Brain Topogr* 29: 218–231.
- Zhu M, Zhang W, Dickens DL, Ding L (2014): Reconstructing spatially extended brain sources via enforcing multiple transform sparseness. *NeuroImage* 86:280–293.